Geosci. Model Dev. Discuss., https://doi.org/10.5194/gmd-2018-119
Manuscript under review for journal Geosci. Model Dev.
Discussion started: 14 June 2018

Geoscientific Model Development Discussions
Open Access
EGU

Evaluation of Monte Carlo tools for high energy atmospheric physics II : relativistic runaway electron avalanches

David Sarria[1], Casper Rutjes[2], Gabriel Diniz[2,3], Alejandro Luque[4], Kevin M. A. Ihaddadene[5], Joseph R. Dwyer[5], Nikolai Østgaard[1], Alexander B. Skeltved[1], Ivan S. Ferreira[3], and Ute Ebert[2,6]

[1]Birkeland Centre for Space Science, Department of Physics and Technology, University of Bergen, Bergen, Norway
[2]Centrum Wiskunde & Informatica (CWI), Amsterdam, The Netherlands
[3]Instituto de Física, Universidade de Brasília, Brazil
[4]Instituto de Astrofísica de Andalucía (IAA-CSIC), P.O. Box 3004, Granada, Spain
[5]University of New Hampshire Main Campus, Department of Physics, Durham, NH, United States
[6]Eindhoven University of Technology, Eindhoven, The Netherlands

Correspondence to: David Sarria (david.sarria@uib.no)

Abstract.

The emerging field of High Energy Atmospheric Physics studies events producing high energy particles and associated with thunderstorms, such as terrestrial gamma-ray flashes and gamma-ray glows. Understanding these phenomena requires appropriate models of the interaction of electrons, positrons and photons with air and electric fields. This work is made as a continuation of Rutjes et al. (2016), now including the effects of electric fields. We investigated results of three codes used in the community (Geant4, GRRR and REAM), for simulating the process of Relativistic Runaway Electron Avalanches. From analytical considerations, we show that the avalanche is mainly driven by electric fields and the ionisation and scattering processes determining the minimum energy of electrons that can runaway.

To investigate this point further, we used a first simulation set-up to estimate the probability to produce a RREA from a relevant range of electron energies and electric field magnitudes. We found that the stepping methodology is important, and the stepping parameters have to be set up very carefully for Geant4. For example, a too large step size can lead to an avalanche probability reduced by a factor of 10, or a 40% over-estimation of the average electron energy. Furthermore, the probability for the particles below 10 keV to accelerate and participate in the penetrating radiation is actually negligible for the full range of electric field we tested ($E < 3$ MV/m). The added value of using models able to accurately track low energy particles (< 10 keV) is minor, and is mainly visible for high E-fields ($E > 2$ MV/m).

In a second simulation set-up, we compared the physical characteristics of the avalanches produced by the four models : avalanche (time and length) scales, time to self-similar state and photon/electron energy spectra. The two Geant4 models and REAM showed a good agreement on all the parameters we tested. GRRR also was also found to be consistent with the other codes, except for the electron energy spectra. That is probably because GRRR does not include straggling for the radiative and ionisation energy losses, hence implementing these two processes is of primary importance to produce accurate RREA spectra. Including precise modelling of the interactions of particles below 10 keV (e.g. taking into account molecular binding energy of secondary electrons for impact ionisation) also provided small differences in the recorded spectra.

Geosci. Model Dev. Discuss., https://doi.org/10.5194/gmd-2018-119
Manuscript under review for journal Geosci. Model Dev.
Discussion started: 14 June 2018

Geoscientific Model Development Discussions
Open Access
EGU

1 Introduction

1.1 Phenomena and observations in high energy atmospheric physics

Wilson (1925) had the conceptual awareness of the generation of high energy radiation from thunderclouds, already 60 years before contemporary theoretical publications and observational results (Williams, 2010). Traditionally, thunderclouds have been studied by classical electromagnetism, but understanding the production and propagation of high energy radiation from thunderstorms falls in the context of High Energy Atmospheric Physics (HEAP). A review is provided by Dwyer et al. (2012). Two space missions specifically designed to study HEAP related phenomena will be available in the years 2018-2019 : ASIM (Atmosphere-Space Interaction Monitor) (Neubert et al., 2006), successfully launched in April 2018; and TARANIS (Tool for the Analysis of Radiation from lightning and Sprites) (Lefeuvre et al., 2009; Sarria et al., 2017).

Observationally different penetrating radiation types have been identified coming from thunderclouds, naturally categorized by duration. Microsecond-long burst of photons, which were first observed from space (Fishman et al., 1994; Briggs et al., 2010), are known as Terrestrial Gamma-ray Flashes (TGF). TGF produces bursts of electron positron pairs (Dwyer et al., 2008; Briggs et al., 2011; Sarria et al., 2016) that follow the geomagnetic field lines into space. Seconds to minutes or even hours long of penetrating X and gamma radiation have been observed on ground, from balloons and aircraft, by McCarthy and Parks (1985); Eack et al. (1996); Torii et al. (2002); Tsuchiya et al. (2007); Adachi et al. (2008); Chilingarian et al. (2010, 2011); Kelley et al. (2015); Kochkin et al. (2017), which are called gamma-ray glows or thunderstorm ground enhancements. In between, on the millisecond duration, a new radiation mechanism has been introduced as TGF afterglows by Rutjes et al. (2017) and measured by Bowers et al. (2017); Teruaki et al. (2017), based on the intermediate neutrons produced by a TGF, creating a prolonged and relocated signal.

Following the idea of Wilson (1925), penetrating radiation is created by runaway electrons, which may further grow by the effect of Møller scattering in the form of so called relativistic runaway electron avalanches (RREA) (Gurevich et al., 1992). The difference in duration between TGF and gamma-ray glows can be explained by two possible different scenario to create runaway electrons, which traditionally is illustrated using the average energy-loss or friction curve. In this curve, there is a maximum at around $\varepsilon \approx 130$ eV, illustrating the scenario that for electric fields higher than the critical electric field, of maximally $E_c \approx 26$ MV/m at standard temperature and pressure (STP), thermal electrons can be accelerated into runaway regime, described in the so-called Cold Runaway theory (Gurevich, 1961). The effective value of E_c may be significantly lower, as electrons could overcome the friction barrier due to their intrinsic random interactions (Lehtinen et al., 1999; Li et al., 2009; Liu et al., 2016; Chanrion et al., 2016). Cold Runaway could happen in the streamer phase (Moss et al., 2006; Li et al., 2009; Chanrion and Neubert, 2010; Köhn and Ebert, 2015) or leader phase (Celestin and Pasko, 2011; Celestin et al., 2012; Chanrion et al., 2014; Kohn et al., 2014; Köhn et al., 2017) of a transient discharge, explaining the high energy electron seeding that will evolve to RREA and produce gamma-rays by bremsstrahlung emission from the accelerated electrons. Alternatively, the relativistic feedback discharge model is also proposed to explain TGF production using large scale and high potential electric fields (Dwyer, 2012), where the RREA initial seeding may be provided by cosmic-ray secondaries, background radiation, or cold runaway (Dwyer, 2008; Celestin and Pasko, 2011)

Geosci. Model Dev. Discuss., https://doi.org/10.5194/gmd-2018-119
Manuscript under review for journal Geosci. Model Dev.
Discussion started: 14 June 2018

Geoscientific Model Development Discussions

For fields significantly below the critical electric field E_c but above the RREA threshold electric field of $E_{\rm rb} = 0.28$ MV/m (at STP), runaway behaviour is still observed in detailed Monte Carlo studies (Dwyer et al., 2012). At thundercloud altitudes, cosmic particles create energetic electrons that could runaway in patches of the thundercloud where the electric field satisfies this criterion. RREA are then formed if space permits and could be sustained with feedback of photons and positrons creating new avalanches (Babich et al., 2005; Dwyer, 2007, 2012). Gamma-ray glows could be explained by this mechanism, as they are observed irrespectively of lighting or observed to be terminated by lightning (McCarthy and Parks, 1985; Chilingarian et al., 2015; Kelley et al., 2015; Kochkin et al., 2017). The fact that gamma-ray glows are not (necessarily) accompanied by classical discharges, results in the conclusion that the electric fields causing gamma-ray glows are usually also below conventional breakdown. The classical breakdown field, of $E_k \approx 3.2$ MV/m at STP, is where low energy electrons (< 200 eV) exponentially grow in number as ionisation overcomes attachment. In this work we focus on electric fields above RREA threshold $E_{\rm rb} = 0.28$ MV/m and below classical breakdown $E_k \approx 3.2$ MV/m to investigate RREA responsible for Terrestrial Gamma-Ray Flashes and gamma-ray glows.

1.2 Theoretical understanding of RREA

In the energy regime of HEAP, the evolution of electrons is driven by electron impact ionisation (Rutjes et al., 2016), as this energy loss channel is much larger than the radiative (bremsstrahlung) energy loss, by a few orders of magnitude. However, this is only true for the average, and bremsstrahlung does have significant effect on the electron spectrum because of straggling Rutjes et al. (2016). For the electron impact ionisation, straggling only occurs for thin targets, as the energy is much more unequally separated (Rutjes et al., 2016). Almost all energy loss of ionisation is going into producing secondary electrons of lower energy ($\epsilon_2 \ll 200$ eV). For this reason it is reasonable to approximate that channel as continuous energy loss or friction because it does not alter the primary electron significantly.

In the case of electric fields above RREA threshold ($E_{\rm rb} = 0.28$ MV/m at STP), there is a possible mode where electrons, when considered as a population, keeps on growing. Some individual electrons do not survive, but the ensemble grows exponentially as new electrons keep being generated. The production of secondaries, above a value much larger than the ionisation threshold, can be approximated by the Møller cross section (which is the exact solution for a free-free electron-electron interaction, e.g. see page 321 of Landau et al. (2013)) multiplied by Z, the number of electrons in the molecule:

$$\begin{aligned}\frac{\mathrm{d}\sigma_{\rm M}}{\mathrm{d}\delta_2} &= Z\frac{2\pi r_e^2}{\gamma_1^2-1}\left[\frac{(\gamma_1-1)^2\gamma_1^2}{\delta_2^2(\gamma_1-1-\delta_2)^2}\right.\\ &- \left.\frac{2\gamma_1^2+2\gamma_1-1}{\delta_2(\gamma_1-1-\delta_2)}+1\right],\end{aligned} \tag{1}$$

where the index $i=1$ indicates the primary electron, $i=2$ the secondary, γ_i the Lorentz factor, $\delta_i = \gamma_i - 1 = \epsilon_i/(m_e c^2)$ the kinetic energy divided by the electron rest energy (with rest mass m_e) and $r_e = \frac{1}{4\pi\epsilon_0}\frac{e^2}{m_e c^2} \approx 2.8\times10^{-15}$ m the classical electron radius. In the case $\delta_2 \ll \gamma_1 - 1$ and $\delta_2 \ll 1$, we observe that the term $\propto 1/\delta_2^2$ is dominating. Thus, we can write equation 1 as:

$$\frac{\mathrm{d}\sigma_{\rm M}}{\mathrm{d}\delta_2} \approx Z\frac{2\pi r_e^2}{\beta_1^2}\frac{1}{\delta_2^2}, \tag{2}$$

Geosci. Model Dev. Discuss., https://doi.org/10.5194/gmd-2018-119
Manuscript under review for journal Geosci. Model Dev.
Discussion started: 14 June 2018

with $\beta_1 = v_1/c$ the velocity of the primary particle. Integrating equation (2) from δ_2 to the maximum energy ($\epsilon_1/2$) yields a production rate

$$\sigma_{\text{prod}} \approx Z \frac{2\pi r_e^2}{\beta_1^2} \frac{1}{\delta_2} \propto \frac{1}{\epsilon_2}, \tag{3}$$

using again $\epsilon_2 \ll \epsilon_1$. The remaining sensitivity of σ_{prod} in units of area to the primary particle is given by the the factor β_1^2 which converges strongly to 1 as the mean energy of the primary electrons exceeds 1 MeV. In other words, as the mean energy of the electrons grows towards even more relativistic energies, the production rate σ_{prod} becomes independent of the energy spectrum.

For illustrative purposes, we consider the one dimensional deterministic case, which results in an analytical solution of the electron energy spectrum. We make the system deterministic by assuming that the differential cross section is a delta-function at $\epsilon_2^{\min}$ and use $\Lambda_{\text{prod}} = \frac{1}{N\sigma_{\text{prod}}}$ as the constant collision length, with N the air number density. In other words, every length Λ_{prod} a secondary electron of energy $\epsilon_2^{\min}$ is produced. The derivation below is close to what was presented in Celestin and Pasko (2010); Dwyer et al. (2012); Skeltved et al. (2014) and references therein.

Consider a population of electrons in 1-dimension with space-coordinate z, a homogeneous and constant electric field E above RREA threshold and a friction force $F(\epsilon)$. The minimum energy $\epsilon_2^{\min}$ that can runaway is given by the requirement $F(\epsilon_2^{\min}) > E$, that is to say $\epsilon_2^{\min} = \text{function}(F, E)$ is constant. Assuming that the mean energy of the ensemble is relativistic, results in a constant production rate $\Lambda_{\text{prod}} = \Lambda_{\text{prod}}(\epsilon_{\min})$. Thus, in space, the distribution f_e grows exponentially as,

$$\frac{\partial f_e}{\partial z} = \frac{1}{\Lambda_{\text{prod}}} f_e. \tag{4}$$

While in energy, the differential equation is given by the net force,

$$\frac{\mathrm{d}\epsilon}{\mathrm{d}z} = qE - F(\epsilon). \tag{5}$$

Solving for steady state means,

$$\frac{\mathrm{d}f_e}{\mathrm{d}z} = \frac{\partial f_e}{\partial z} + \frac{\partial f_e}{\partial \epsilon}\frac{\mathrm{d}\epsilon}{\mathrm{d}z} = 0, \tag{6}$$

and using equation 4 and 5 results in,

$$\frac{\partial f_e}{\partial \epsilon} = -\frac{1}{\Lambda_{\text{prod}}(qE - F(\epsilon))} f_e. \tag{7}$$

For the largest part of the energy spectrum, specifically above 0.511 MeV and below 100 MeV, $F(\epsilon)$ is not sensitive to ϵ (e.g. see Rutjes et al. (2016)). Only at around $\epsilon \approx 100$ MeV electron energy $F(\epsilon)$ starts increasing again because of bremsstrahlung. Thus, one may assume $F(\epsilon) \approx F$ constant, which yields that the RREA energy spectrum $f(\epsilon)$ at steady state is given by,

$$f_e(\epsilon) = \frac{1}{\bar{\epsilon}} \exp\left(-\frac{\epsilon}{\bar{\epsilon}}\right), \tag{8}$$

with the exponential shape parameter and approximated average energy $\bar{\epsilon}(E)$ given by,

$$\bar{\epsilon}(E) = \Lambda_{\text{prod}}(qE - F). \tag{9}$$

Geosci. Model Dev. Discuss., https://doi.org/10.5194/gmd-2018-119
Manuscript under review for journal Geosci. Model Dev.
Discussion started: 14 June 2018

Geoscientific Model Development Discussions

Equivalently, in terms of collision frequency $\nu_{\mathrm{prod}} = \frac{\beta c}{\Lambda_{\mathrm{prod}}}$, equation 9 can be written as,

$$\bar{\epsilon}(E) = \frac{\beta c}{\nu_{\mathrm{prod}}}(qE - F), \tag{10}$$

with β the velocity v/c of the RREA avalanche front. For the 1-d case there is no momentum-loss or diffusion, so $\beta \approx 1$. Note that Λ_{prod} depends on $\epsilon_2^{\mathrm{min}} = \epsilon_2^{\mathrm{min}}(E)$, which in turn depends on the electric field E as that determines the minimum electron energy that can go into runaway.With this simple analysis we illustrate with equation 8 and 9, that the full RREA characteristics, such as the mean energy $\bar{\epsilon}$ or the collision length Λ_{prod} (directly related to the avalanche length scale λ discussed in section 4.1) are driven by processes determining $\epsilon_2^{\mathrm{min}}$.

In reality there are important differences compared to the one dimensional deterministic case described previously, which we propose to discuss qualitatively for understanding the Monte Carlo simulations evaluated in this study. During collisions, electrons deviate from the path parallel to E. Therefore in general, electrons experience a reduced net electric field as the cosine function of the opening angle θ, which reduces the net force to $qE\cos(\theta) - F$ and thereby the mean energy $\bar{\epsilon}$ of equation 9. In reality the 3D scattering (with angle parameter θ) changes of the path of the particle. Although the velocity remains still close to c (as the mean energy is still larger than several MeV), the RREA front velocity parallel to E is reduced again because of the opening angle as function of its cosine:

$$\beta_{\parallel} = \beta\cos(\theta), \tag{11}$$

which also reduces the mean energy $\bar{\epsilon}$. Equivalently the avalanche scale length Λ_{prod} in 3-D changes to $\approx \Lambda_{\mathrm{prod}} \times \cos(\theta)$. However, most importantly, the momentum-loss of the lower energetic electrons results in a significant increase of $\epsilon_2^{\mathrm{min}}$, as it is much harder for electrons to runaway. The increase of $\epsilon_2^{\mathrm{min}}$ significantly increases Λ_{prod} and thereby increases the characteristic mean energy $\bar{\epsilon}$. On the other hand, the stochasticity creates a interval of possible energies $\epsilon_2^{\mathrm{min}}$ that can runaway with a certain probability and for thin targets a straggling effect (Rutjes et al., 2016).

The effects discussed above prevent a straight forward analytical derivation of the RREA characteristics in 3 dimensions, but what remains is the important notion that the physics is completely driven by the intermediate energy electron production. Intermediate electrons in the sense they are far above ionisation threshold ($\gg 200$ eV) but much below relativistic energies ($\ll 1$ MeV). The parametrization of the electron energy spectrum, given by equation 9 turns out to be an accurate empirical fit, as it was already shown in Celestin and Pasko (2010); Dwyer et al. (2012); Skeltved et al. (2014) and references therein. Nevertheless in these works $\lambda^{\mathrm{min}}(E)$, or equivalently the velocity over collision frequency $\beta c/\nu_{\mathrm{prod}}$, is fitted by numerical Monte Carlo studies and the final direct relation to $\epsilon_2^{\mathrm{min}}$ is not executed. Celestin and Pasko (2010) calculated that $\nu^{\mathrm{prod}}(E) \propto E$, thus explains why $\bar{\epsilon}(E)$ must saturate to constant value. Celestin and Pasko (2010) argue that $\epsilon_2^{\mathrm{min}}$(E) is given by the deterministic friction curve F, for which they use the Bethe's formula and an integration of a more sophisticated electron impact ionisation cross section (RBEB) including molecular effects, but that is only true in 1-D without stochastic fluctuations. Other attempts to simulate RREA by solving the kinetic equation instead of using Monte-Carlo methods are presented in Roussel-Dupre et al. (1994); Gurevich and Zybin (1998); Babich et al. (2001) and references therein. An analytical approach is provided by Cramer et al. (2014).

Geosci. Model Dev. Discuss., https://doi.org/10.5194/gmd-2018-119
Manuscript under review for journal Geosci. Model Dev.
Discussion started: 14 June 2018

1.3 Model reductions and previous study

The physics behind TGF, TGF afterglows and gamma-ray glows are studied with the help of computer simulations, which necessarily involves model reduction and assumptions. Fortunately, in scenarios where the electric field is below classical breakdown the system can be simplified, because electrons that decelerate and eventually attach will not contribute to the production of the penetrating radiation. In Monte Carlo simulations it is therefore common to apply a so-called "low energy cutoff", a threshold where particles with lower energy can be discarded, to improve code performance (i.e. computation time). A second simplification can be made for the energetic enough particles that stay in the ensemble, by treating collisions that would produce particles below the low energy cutoff as a friction.

Both simplifications can be implemented in different ways, leading to different efficiencies and accuracies. Rutjes et al. (2016) benchmarked the performance of the Monte Carlo codes Geant4 (Agostinelli et al., 2003), EGS5 (Hirayama et al., 2005), FLUKA (Ferrari et al., 2005) developed in other fields of physics, and of the custom-made codes GRRR (Luque, 2014) and MC-PEPTITA (Sarria et al., 2015) within the parameter regime relevant for HEAP, in the absence of electric and magnetic fields. In that study they focused on basic tests of electrons, positrons and photons with kinetic energies between 100 keV and 40 MeV through homogeneous air using a low energy cutoff of 50 keV and found several differences between the codes and invited other researchers to also test their codes on the provided test configurations. Most of the differences revealed that using an average friction fails also in the high energy regime ($\gg 200$ eV), as the energy loss is averaged out too much resulting in an incorrect energy distribution (Rutjes et al., 2016), called the straggling effect.

Since including or not this straggling effect in the simulation is of primary importance for the present study as well, it is worth summarizing what it consists in. This effect was first studied by Bethe and Heitler (1934). If it is not taken into account in the implementation of the low energy cut-off, the primary particle suffers a uniform (and deterministic) energy loss. This means that only the energy of the primary particle is altered, but not its direction. The accuracy of the assumed uniform energy loss is a matter of length scale : on a small length scale, the real energy loss distribution (if all interactions are considered explicitly) among the population would have a large spread. One way to obtain the real energy distribution is by implementing a stochastic friction mimicking the straggling effect.

Rutjes et al. (2016) also indicated that including electric fields in the simulations would potentially enhance the differences found by introducing new errors, the simulation results begins supposingly sensitive to the low energy cutoff. This effect is believed to be responsible of the observed differences between the two Geant4 physics lists test in the comparison study of Skeltved et al. (2014): for all fields between 0.4 and 2.5 MV/m (at STP), they found that energy the spectrum and the mean energy of runaway electrons depended on the low energy cutoff, even when it was chosen between 250 eV and 1 keV. In the present article, this interpretation is challenged.

1.4 Content and order of the present study

In the context of High Energy Atmospheric Physics, the computer codes that were used are either general purpose codes developed by large collaborations, or custom made codes programmed by smaller groups or individuals. Examples of general

Geosci. Model Dev. Discuss., https://doi.org/10.5194/gmd-2018-119
Manuscript under review for journal Geosci. Model Dev.
Discussion started: 14 June 2018

purpose codes that were used are Geant4 (e.g., Østgaard et al., 2008; Carlson et al., 2010; Bowers et al., 2017; Sarria et al., 2015, 2017; Skeltved et al., 2014) and FLUKA (e.g., Dubinova et al., 2015; Rutjes et al., 2017). Custom made codes were used in Lehtinen et al. (1999); Dwyer (2003); Østgaard et al. (2008); Celestin and Pasko (2011); Luque (2014); Kohn et al. (2014); Chanrion et al. (2014); Sarria et al. (2015), among others. Rutjes et al. (2016) presented in their section 1.3 the reasons why different results between codes (or models) can be obtained and why defining a comparison standard (based on the physical outputs produced by the codes) is the easiest way (if not the only) to compare and validate the codes. Here we continue the work of Rutjes et al. (2016), to provide a comparison standard for the particle codes able to simulate Relativistic Runaway Electron Avalanches, as simple and informative as possible, by only considering their physical outputs. These comparison standards are extensively described in the Supplementary Material (Sections 1 and 2).

To prove our new insights, and to benchmark codes capable of computing RREA characteristics for further use, we calculated the probability for an electron to accelerate into the runaway regime (see section 3), which is closely related to the quantity $\epsilon_2^{\min}(E)$. From this probability study, it is directly clear that it is safe to choose the low energy cutoff ε_c higher than previously expected by Skeltved et al. (2014) and Rutjes et al. (2016), even higher than $F(\varepsilon_c) > E$ given an electric field $E < E_k$. The probability for these particles below ε_c to accelerate and participate in the penetrating radiation is actually negligible. In practice an energy threshold value of about $\varepsilon_c = 10$ keV can be used for any electric field below the conventional breakdown field. Nevertheless, we found out that step-length restrictions are of major importance (e.g. it can lead to a factor of 10 underestimation of the probability to produce a RREA), as will be described in section 2.4. The results of the comparison of several parameters of the RREA produced by the four tested codes is then presented in section 4.3. We conclude in section 5.

The test set-ups of both simulations (RREA probability, and RREA characteristics) are described in detail in the Supplementary Material, together with data we obtained, and figures comparing several different characteristics.

2 Model descriptions

For this work, the data we discuss in the next sections was provided by the general-purpose code Geant4 (with several set-ups) and two custom-made codes (GRRR and REAM) which we describe below.

2.1 Geant4

Geant4 is a software toolkit developed by the European Organization for Nuclear Research (CERN) and a worldwide collaboration (Agostinelli et al., 2003; Allison et al., 2006, 2016). We use version 10.2.3. The electro-magnetic models can simulate the propagation of photons, electrons and positrons including all the relevant processes, and the effect of electric and magnetic fields. Geant4 uses steps in distance, whereas REAM and GRRR use time step. In the context of this study, three main different electro-magnetic cross-section sets implementation are included : one based on analytical of semi-analytical models (e.g. uses the Møller cross section for ionisation and Klein-Nishina cross section for Compton scattering), one based on the Livermore data set (Perkins et al., 1991), and one based on the Penelope models (Salvat et al., 2011). Each of them can be implemented

Geosci. Model Dev. Discuss., https://doi.org/10.5194/gmd-2018-119
Manuscript under review for journal Geosci. Model Dev.
Discussion started: 14 June 2018

Geoscientific Model Development Discussions

with a large number of different electro-magnetic parameters (binning of the cross section tables, energy thresholds, production cuts, maximum energies, multiple scattering factors, accuracy of the electro-magnetic field stepper, among others), and some processes have multiple models in addition to the main three, e.g. the Monash University model for Compton scattering (Brown et al., 2014). Skeltved et al. (2014) used two different physics list : LHEP and LBE. The first one, based on parametrization on measurement data and optimized for speed, was deprecated since the 10.0 version of the toolkit. The LBE physics list is based on the Livermore data, but it is not considered as the most accurate electro-magnetic physics list in the Geant4 documentation, which is given by the Option 4 physics list (O4). This last uses a mix of different models, and in particular uses the Penelope model for the the impact ionisation of electrons. For this study, we will use two GEANT4 physics list options : Option 4 (referred as simply O4 hereafter) that is the most accurate one according to the documentation, and the Option 1 (referred as simply O1 hereafter) that is less accurate, but runs faster. In practice, O1 and O4 give very similar results for simulations without electric field and energies above 50 keV, as produced in our previous code comparison study (Rutjes et al., 2016).

Concerning how low the energy threshold is handled, Geant4, by default, is following all primary particles down to zero energy. A primary particle is defined as a particle with more energy than a threshold energy ϵ_c^p (that is different from ϵ_c described before). The default ϵ_c^p is set to 990 eV and is not changed in this study. The LBE Physics list used in (Skeltved et al., 2014) uses a threshold down to 250 eV, and this parameters was thought to be responsible major change in the simulated RREA energy spectra. In section 3, we will argue that the main parameter governing the spectrum is the accuracy of the stepping method for the tracking of the particles. The interpretation of (Skeltved et al., 2014) was possible because reducing the value of ϵ_c^p also indirectly reduces the average step that is used by the simulation.

2.2 GRRR

The GRRR (GRanada Relativistic Runaway simulator) is a time-oriented code for the simulation of energetic electrons propagating in air, and can handle self-consistent electric fields. It is described in detail in the supplement of Luque (2014) and its source code is fully available in a public repository (see section 7 about code availability). In the scope of this work, we want to point out three important features : 1. Electron ionisation and scattering processes are simulated discretely, and the friction is uniform and without a way to mimic the straggling effect. 2. Bremsstrahlung collisions are not explicit and are simulated as continuous radiative losses, without straggling. 3. GRRR uses a constant time-step Δt both for the integration of the continuous interactions using a fourth-order Runge-Kutta scheme and for determining the collision probability of each discrete process k as $\nu_k \Delta t$, where ν_k is the collision rate of process k. This expression assumes that $\nu_k \Delta t \ll 1$ and therefore that the probability of a particle experiencing two collisions within Δt is negligibly small. The collisions are sampled at the beginning of each time step and therefore the rate ν_k is calculated using the energy at that instant. In this work we used $\Delta t = 0.25$ ps for the avalanche probabilities simulations, and $\Delta t = 1$ ps for the simulations used to characterise the RREA. For both cases, the time steps are small enough to guarantee a very accurate integration.

Geosci. Model Dev. Discuss., https://doi.org/10.5194/gmd-2018-119
Manuscript under review for journal Geosci. Model Dev.
Discussion started: 14 June 2018

2.3 REAM

The REAM (Runaway Electron Avalanche Model) is a three dimension Monte Carlo simulation of Relativistic Runaway Electron Avalanche (also refereed as Runaway Breakdown), including electric and magnetic fields (Dwyer, 2003, 2007; Cramer et al., 2016). This code is inspired by earlier work by Lehtinen et al. (1999) and takes accurately into account all the important interactions involving runaway electrons, including energy losses through ionisation, atomic excitation and Møller scattering. A shielded-Coulomb potential is implemented in order to fully model elastic scattering, and it also includes the production of X/gamma-rays from radiation energy loss (bremsstrahlung) and the propagation of the photons, by including photoelectric absorption, Compton scattering and electron/positron pair production. The positron propagation is also simulated, including the generation of energetic seed electrons through Bhabha scattering. The bremsstrahlung photon emissions from the newly produced electrons and positron are also included.

In the scope of this study, it is important to point out that REAM limits the time step size of the particles so that the energy change within one time step cannot be more than 10 %. The effect of reducing this factor down to 1 % was tested and did not make any noticeable difference in the resulting spectra. The comparative curves are presented in the Supplementary Material, section 4.

2.4 Stepping methodology

2.4.1 General method

In Monte Carlo simulations, particles propagate in steps, collide and interact with surrounding media by means of cross sections (and their derivatives). A step is defined by the displacement of a particle between two collisions. As it is presented in sections 3 and 4, this stepping methodology is responsible for most of the differences we observed between the codes we tested. Simulations can be either *space-oriented* or *time-oriented*, if the stepping is done in space or in time. By construction, space-oriented simulations are thus not synchronous in time. Usually, a single particle is simulated over its entire life-time before going to the next particle. The advantage of asynchronous simulations is the ability to easily include boundaries, to have particles step as far as possible in the same material (minimizing the overhead due to null collisions), and smaller memory usage since there is no need to store all the particles alive at a given time (that may be a million or more). However, asynchronous simulations makes it impossible to incorporate particle to particle interactions, such as a space charge electric field.

During steps, charged particles can loose energy (and momentum) by collisions, and also change in energy (and momentum) when an electric fields is present. To guarantee accuracy, energies should be updated frequently enough. An accurate method would be to exponentially sample step lengths with

$$\delta\ell = \min_{\epsilon}\{(\sigma_t(\epsilon)N)^{-1}\}, \tag{12}$$

in space-oriented perspective, or

$$\delta t = \min_{\epsilon}\{(v(\epsilon)\sigma_t(\epsilon)N)^{-1}\}, \tag{13}$$

Geosci. Model Dev. Discuss., https://doi.org/10.5194/gmd-2018-119
Manuscript under review for journal Geosci. Model Dev.
Discussion started: 14 June 2018

in time-oriented perspective. With v the velocity, σ_t the total cross section and N the number density of the medium. Then at each updated location (and energy), the type of collision must be sampled from probability distributions. The probability of doing a collision of the given process (pr) can be calculated with:

$$p_{pr} = 1 - \exp\left(-N \int_i^f \sigma_{pr}\left(\epsilon(\ell)\right)\, d\ell\right) \tag{14}$$

Where the index i refers to the beginning of the step, f to its end, ℓ is the step length variable along the trajectory, and $d\ell$ is an infinitesimal step length. For time oriented simulations, we have equivalently :

$$p_{pr} = 1 - \exp\left(-N \int_i^f v(\epsilon(t))\,\sigma_{pr}\left(\epsilon(t)\right)\, dt\right) \tag{15}$$

Using these probabilities along a given step length or duration, there is a chance that no interactions happens, but the energy of the particle is guaranteed to be updated correctly.

2.4.2 The case of Geant4

In the Geant4 documentation, the stepping method presented in the previous section is referred as the "the integral approach to particle transport". This method is set up by default in Geant4 for impact ionisation and bremsstrahlung. However, the way it is implemented is not exactly following what was described in previous section. The description of the exact implementation is out of the scope of this article, but is presented into details in Ivanchenko et al. (1991) and Apostolakis et al. (2009). The method relies on determining the maximum of the cross section over the step (σ_{max}), using a parameter ξ, that is based on another parameter α_R, that is also used to determine the step lengths. Another related parameter is the maximum range parameter (ρ_{max}), set to the default values of 1 millimeter and 0.1 millimeter for O1 and O4 respectively, and was never changed in the scope of this study. The exact definition of these parameters is given in Allison et al. (2016) and in the online Geant4 documentation (available at http://geant4.cern.ch/support/userdocuments.shtml). The default value of α_R is set to 0.80 for O1 and to 0.20 for O4. We found out that both values are not low enough to be able to produce accurate results for the RREA probability simulations presented in the next section. To make Geant4 able to produce accurate RREA simulations, two methods are possible.

The first method is to tweak the value of the α_R parameter. Its value is set to 0.80 by default for O1, and 0.20 by default for O4. We found that these default values are way too high to be able to produce accurate RREA simulations, and values of $\alpha_R < 5.0 \times 10^{-3}$ should be used, as presented in the next section.

The second method is to implement a step limiter process (or maximum acceptable step). By default, this max step ($\delta\ell_{max}$) is set to one kilometer, and such a large value has no effect in practice, since the mean free path of energetic electrons in STP air is orders of magnitude smaller. Acceptable values of $\delta\ell_{max}$ depend on the electric field, and we found out that it should be

Geosci. Model Dev. Discuss., https://doi.org/10.5194/gmd-2018-119
Manuscript under review for journal Geosci. Model Dev.
Discussion started: 14 June 2018

Geoscientific Model Development Discussions

set to 1 millimeter or less to produce accurate RREA simulations, as presented in the next section. However, using this method results in relatively long simulation time required to achieve an acceptable accuracy, as the step is not adapted to the energy of the electrons. For information, the relative impact on performance (in terms of requirements of computation time) of tweaking the $\delta\ell_{max}$ and α_R parameters is presented in Appendix A.

3 Probability of generating RREA

As a first comparison test, we estimated the probability for an electron to accelerate into the runaway regime and produce a RREA, given its initial energy ϵ and some electric field magnitude E. We defined this probability as the fraction of initial (seed) electrons that created an avalanche of at least 20 electrons above 1 MeV. Once this state is reached, there is no doubt the RREA is triggered and can go on forever if no limits are set. The number 20 is arbitrary, to be well above 1 but small enough for computational reasons. For some initial conditions, we also tested requirements of 30 and 50 electrons above 1 MeV, that resulted in very similar probabilities. This study is somehow similar to the works presented in Lehtinen et al. (1999); Li et al. (2009); Liu et al. (2016); Chanrion et al. (2016), but they all looked at the probability to have only one single runaway electron, whereas we used the criterion of 20 electrons above 1 MeV, that is a stricter constraint. The difference between the two criteria is mainly noticeable for low electric field (< 0.4 MV/m) and high seed energies (> 700 keV).

As a test case, we calculated the probability to produce RREA as function of α_R and $\delta\ell_{max}$ (these parameters are presented in the previous section), for the configuration $\epsilon = 75$ keV, $E = 0.80$ MV/m. The results are presented in figure 1. Although this configuration has a very low RREA probability for O1/O4 by default (where α_R respectively equal to 0.80 and 0.20, and $\delta\ell_{max}$ is one kilometer for both), the probability increases as α_R decreases and converges to a value between 10 and 12 % for both models when $\alpha_R < 5.0 \times 10^{-3}$. The same effect is observed when reducing $\delta\ell_{max}$. In this case, the user should not set $\delta\ell_{max}$ below the maximum range parameter, set to 1 millimeter for O1 and 0.1 millimeter for O4 by default (never changed in the scope of this article). When reducing the α_R parameter to arbitrarily small values, both Geant4 models converge to slightly different probabilities : 10.7 % for O1 and 11.7 % for O4. We think this small difference is not due to the stepping method, as reducing ρ_{max} or α_R further does not produce a significant difference. It is probability due to other factors, in particular the difference in the physical models and cross section sets used.

As explained in section 1.2, the final electron spectrum is essentially driven by the minimum energy $\epsilon_2^{\min}$ of electrons that can create a RREA. Here we can clearly see this probability is strongly affected by the choice of the α_R and $\delta\ell_{max}$ simulation parameters, affecting the accuracy of the stepping method, and that the values set by default for these parameters are not correct for correctly handling this problem.

In figure 2, we compare the contour lines of the 10%, 50% and 90% probability of triggering a RREA as function ϵ and E, for three codes : Geant4 O4 ($\alpha_R = 1.0 \times 10^{-3}$), Geant4 O1 ($\alpha_R = 1.0 \times 10^{-3}$) and GRRR. For most of the domain, the level curves are consistent between O1, O4 and GRRR. The most important difference is present for energies > 200 keV and low E-field (< 0.5 MV/m). At 1 MeV, the level curves are quite significantly different between the Geant4 models and GRRR: the 50% probability to trigger RREA for GRRR is approximately located at the 10 % probability for O4, and the 90 % probability

Geosci. Model Dev. Discuss., https://doi.org/10.5194/gmd-2018-119
Manuscript under review for journal Geosci. Model Dev.
Discussion started: 14 June 2018

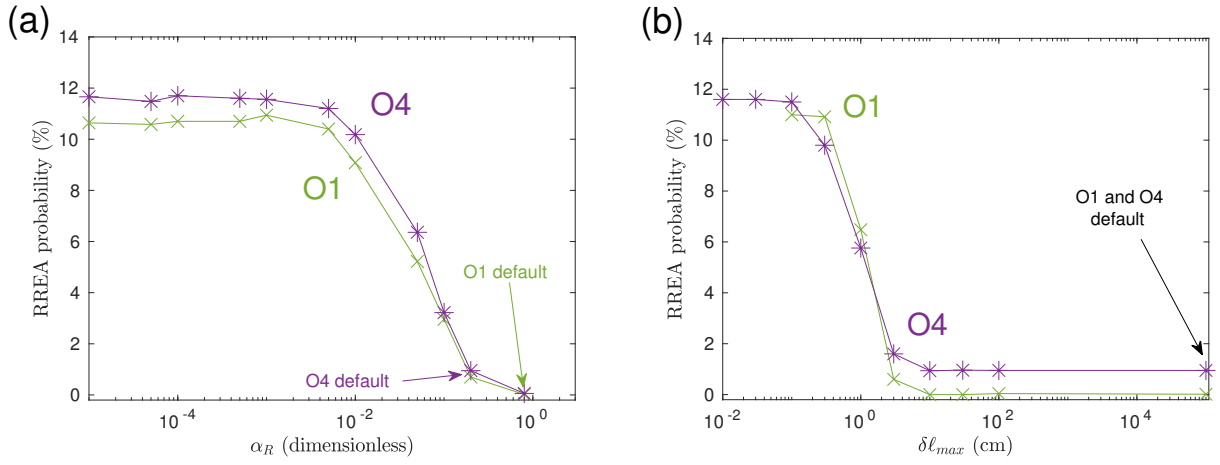

Figure 1. Relativistic avalanches probabilities calculated from Geant4 simulations, for specific point $\{\epsilon = 75\ \mathrm{keV}, \mathrm{E} = 0.80\ \mathrm{MV/m}\}$ (illustrated by a cross in figure 2) and for two stepping settings. **(a)** : Avalanche probability versus α_R setting for Geant4 O4 and Geant4 O1. **(b)** : Avalanche probability versus maximum step setting ($\delta\ell_{max}$) for Geant4 O4 and Geant4 O1.

to for GRRR is located at the 50 % probability for O1. The reason is probably similar to a point we raised in our previous study (Rutjes et al., 2016) : GRRR does not include a way to simulate the straggling effect for the ionisation process. By looking at figure 2 of Rutjes et al. (2016), we can see that 200 keV is roughly the energy from where the difference in the spectrum of GRRR, compared to codes that simulate straggling, starts to become significant.

For low electron energy (< 40 keV) and high electric field (> 2 MV/m), GRRR and O4 present a good agreement, however O1 deviates significantly from O4. We double checked the effects of the stepping parameters (α_R, $\delta\ell_{max}$ and ρ_{max}) and it is clear that they were not involved in this case. We think the Møller differential cross section (with respect to the energy of the secondary electron) used by O1 and extrapolated down to low energies leads to the production of secondary electrons with average energies lower than the Penelope model (used by O4), that includes the effects of the atomic electron shells, hence is probably more accurate. This hypothesis is confirmed by looking at the shape of the differential cross sections of impact ionisation, which plots are presented in the Supplementary Material, section 8.4.

4 Characteristisation of RREA showers

We compared the output of the four models over 12 different electric field magnitudes from $E = 0.60$ MV/m to $E = 2.8$ MV/m. Two types of simulation were set : record in time, and record in distance (or space). This last choice was made because the resulting spectra can change significantly depending on the record method, as presented in figure 10 of Skeltved et al. (2014). All the curves presenting the simulation results are presented in the Supplementary Material, as well as the complete details on how the simulation should be set up. In the following section, we discuss only the most important differences we found between the four codes. We show the comparison of avalanche scales in space and time in section 4.1 and in section 4.2 the

Geosci. Model Dev. Discuss., https://doi.org/10.5194/gmd-2018-119
Manuscript under review for journal Geosci. Model Dev.
Discussion started: 14 June 2018

Geoscientific Model Development Discussions
Open Access
EGU

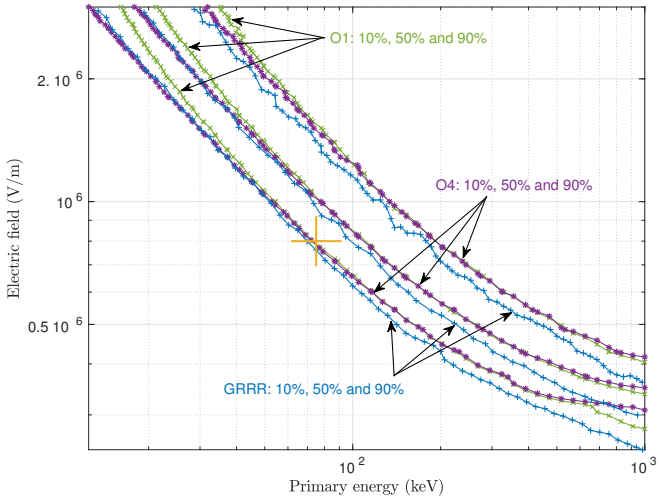

Figure 2. Avalanche probability comparison between O4, O1 and GRRR, with three contour probabilities 10%, 50% and 90%. These contours are derived from the full probability scan, that are presented in the Supplementary Material. The cross at $\{\epsilon = 75\ \mathrm{keV}, \mathrm{E} = 0.80\ \mathrm{MV/m}\}$ highlights the point where we studied the behaviour of the stepping simulation parameters for the O4 and O1 the probability, see figure 1.

evolution to self-similar state. Finally, in section 4.3 we show the comparison of the self-similar energy spectra of electrons and photons of the RREA.

4.1 Avalanche time and length scales

Figure 3 and 4 show the avalanche length and time scales as function of electric fields, for the four models, together with their relative difference with respect to REAM. Note that we could not compute any values for electric fields below 0.60 MV/m, as we used only 200 initial electron seeds of 100 keV, which have a very low probability to trigger RREA for such fields. All the models agree well, within $\pm 10\%$. There is also a systematic shift of about 7 % between the two Geant4 models for both time and length scales. The Geant4 O4 model is in principle more accurate than the O1 model, since it includes more advanced models. For most of the electric fields, O1 tends to be closer to REAM and O4 tends to be closer to GRRR. Following Coleman and Dwyer (2006), the avalanche length and time can be fitted by the empirical models,

$$\lambda(E) = \frac{c_1}{E - c_2}, \tag{16}$$

$$\tau(E) = \frac{c_3}{E - c_4} \tag{17}$$

where c_1 is in V, c_2 and c_4 in V/m and and c_3 in s.V/m. The c_2 and c_4 parameters can be seen as two estimates of the magnitude of the electric field of the minimum of ionisation for electrons along the avalanche direction, and also of the electric field

Geosci. Model Dev. Discuss., https://doi.org/10.5194/gmd-2018-119
Manuscript under review for journal Geosci. Model Dev.
Discussion started: 14 June 2018

magnitude of the RREA threshold; both values being close. However, we note that these fits neglect the sensitivity of the mean energy and velocity to the electric field. These empirical fits are motivated from the relations presented in equation 9 and 10, derived for the one dimensional case. First results of such fits were presented in Coleman and Dwyer (2006). The best fit values of the two models to the simulation data are given in table 1. The c_1 parameter is directly linked to the average energy of the RREA spectrum, though the definition of this average energy can be ambiguous as energy spectra change significantly if recorded in time or in space. The values given by all the code are located between 6.8 and 7.61 MV, and are all consistent with each other within a 95 % confidence interval, with the exception of O4 that slightly deviates from O1. Combining all the values gives :

$$\overline{c_1} = 7.28 \pm 0.10 \text{ MV} \tag{18}$$

That is consistent with the value of 7.3 ± 0.06 MV given in Coleman and Dwyer (2006). And all the estimated values of the c_2 and c_4 are consistent with each other within a 95 % confidence interval. Combining all the values of c_2 and c_4 gives :

$$\overline{c_2} = 279 \pm 5.6 \text{ kV/m}$$
$$\overline{c_4} = 288 \pm 4.8 \text{ kV/m}$$

And both value are also consistent with each other, leading to the final value of $\overline{c_{2,4}} = 283.5 \pm 3.69$ kV/m. These values slightly deviates from the value of 276.5 ± 2.24 obtained from Coleman and Dwyer (2006) if the values they obtained for the fits of λ and τ are combined. The work of Coleman and Dwyer (2006) used the REAM model too, in a version that should not have significantly changed compared to the one used here. Thus, we think this difference is purely attributed to differences in the methodology that was used to make these estimates from the output data of the code. Concerning the c_3 parameter, combining all the estimates gives $\overline{c_3} = 26.8 \pm 0.32$ ns MV/m, that is slightly lower the value of 27.3 ± 0.1 ns MV/m of Coleman and Dwyer (2006), but none of the values are consistent within the 95 % confidence interval. For this case, we also think the slight difference can be attributed to differences in methodology. Furthermore, the ratio $\overline{c_1}/\overline{c_3}$ can also be used to determine an average speed of the avalanche $\approx \beta_{\parallel} c$, and we can estimate $\beta_{\parallel} \approx 0.90$, that is very close to what was found in previous studies.

4.2 Evolution to self-similar state

The photon and electron energy spectra of relativistic runaway electron avalanche (RREA) is known to converge in time to a self-similar solution, where its shape is not evolving anymore, even if the number of particles continues growing exponentially. It may also be referred as the "self-sustained state", or the "steady state" in the literature. At least 5 avalanche lengths (or avalanche times) are required to be able to reasonably assert that this state is reached. We propose to estimate this time by looking to the mean electron energy evolution as function of time. Notice that, as already mentioned in the beginning of Section 4, this mean energy recorded in time is different from the one recorded in distance, used in the next section. We arbitrarily choose to evaluate this mean by averaging all the energy of each individually recorded electrons from 10 keV and

Geosci. Model Dev. Discuss., https://doi.org/10.5194/gmd-2018-119
Manuscript under review for journal Geosci. Model Dev.
Discussion started: 14 June 2018

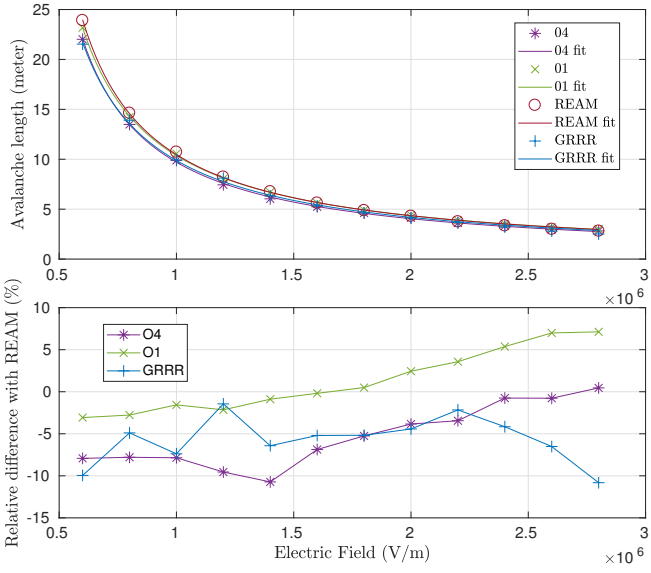

Figure 3. Top : Avalanche multiplication length as function of ambient electric field, for each of the codes included in this study. **Bottom** : The relative difference of all other models with respect to REAM. Table 1 indicates the values of the fit parameters.

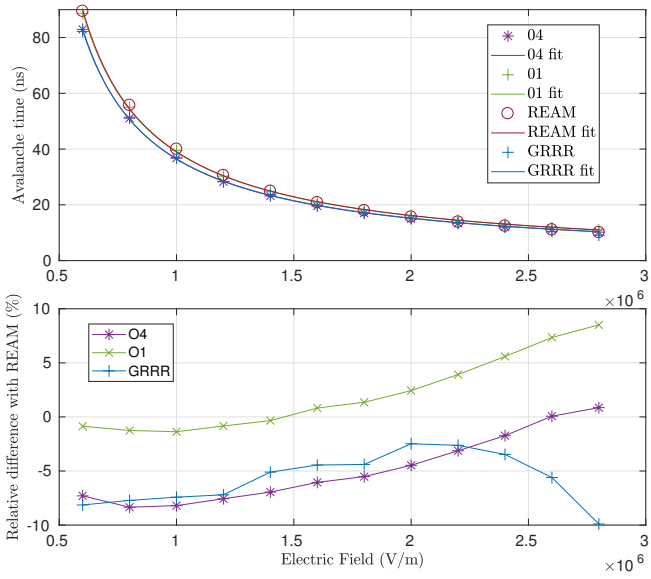

Figure 4. Top : Avalanche multiplication time as function of ambient electric field, for each of the codes included in this study. **Bottom** : The relative difference of all other models with respect to REAM. Table 1 indicates the values of the fit parameters.

Geosci. Model Dev. Discuss., https://doi.org/10.5194/gmd-2018-119
Manuscript under review for journal Geosci. Model Dev.
Discussion started: 14 June 2018

Geoscientific Model Development Discussions
Open Access
EGU

Table 1. Values of the parameters of the fits (with 95 % confidence intervals) for the simulations data for avalanche scale in space and time, using the models described by equations 16 and 17. See figure 3 and 4 for the corresponding curves.

Code	Avalanche length		Avalanche time	
	c_1 (MV)	c_2 (kV/m)	c_3 (ns MV/m)	c_4 (kV/m)
REAM	7.43 ± 0.18	290 ± 9.5	27.6 ± 0.91	293 ± 13
G4 O1	7.50 ± 0.10	276 ± 5.6	27.6 ± 0.44	290 ± 6.3
G4 O4	6.93 ± 0.13	285 ± 7.5	25.9 ± 0.28	288 ± 4.2
GRRR	7.25 ± 0.30	266 ± 18	26.2 ± 0.76	282 ± 12

above. This choice of a 10 keV energy threshold (instead of a higher value, like 511 keV or 1 MeV) does not affect significantly the final estimate of this time to self-similar state. We started with a mono-energetic beam of 100 keV electrons, which are considered low enough compared to the self-similar state mean energy of 6 to 9 MeV. To define the time to self-similar state (T_s), we fitted the time evolution of the mean electron energy $\bar{\epsilon}$ with the model

$$\bar{\epsilon}(t) = b_1 - b_2 \times \exp(-t/b_3), \tag{19}$$

where b_1 and b_2 have dimension of energy, b_3 dimension of time, and we define $T_\mathrm{s} = 5\, b_3$, that is five e-folding times, i.e. converged to 99.3%. The evolution of electrons spectra to self-similar state are illustrated for the Geant4 O4 model in the supplementary material (section 11.4). The values of T_s we estimated for the different models are presented in figure 5, together with relative differences of the models with respect to REAM. The relatively high uncertainty (within 95 % confidence intervals) that can be seen on the estimate of T_s is due to a combination of the confidence interval from the exponential fit, from the statistics of the number of seed electrons that could produce a RREA, and from the statistics of the particle counts. For most case, 200 initial seed were used, but for REAM, only 16 seeds were simulated for $E \geq 2.2$ MV/m, and for GRRR, only 20 seeds were simulated above $E \geq 2.0$ MV/m, because of computation time limitations.

In figure 5, Geant O1, O4, GRRR and REAM show consistent times to reach the self-similar state, for all the E-fields. Notice that for them, $T(= T_\mathrm{s}/5)$ is close to the avalanche time value τ given in the top panel of figure 4. For the low electric field of 0.60 MV/m, it seems to take about 5 times more to reach self-similar state. For this field, there were only three electrons seeds that could produce a RREA, giving a large uncertainty on the estimate of T_s, making it impossible to conclude on an inconsistency. From 0.60 MV/m to 1.8 MV/m, where all data from codes have good statistics, the times to self-similar state are consistent. From 2.0 MV/m to 2.4 MV/m, the two Geant4 models and REAM are consistent, but GRRR present lower times by about -20% to -50 %, but it is impossible to conclude to an inconsistency, given the large confidence intervals. For E-field magnitudes of 2.6 MV/m to 2.8 MV/m, O1 and O4 present times to self-similar state lower than REAM by about 50 %, that is significant given the uncertainty intervals, whereas GRRR and REAM are consistent. We could not find a clear explanation for it.

Geosci. Model Dev. Discuss., https://doi.org/10.5194/gmd-2018-119
Manuscript under review for journal Geosci. Model Dev.
Discussion started: 14 June 2018

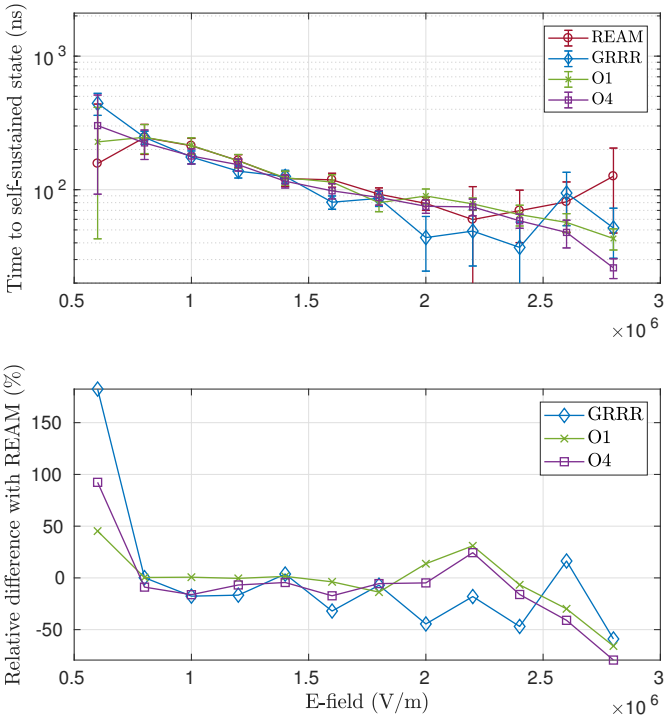

Figure 5. Top : time to self-similar state as function of ambient electric field, for each of the codes included in this study. **Bottom** : relative difference with respect to REAM.

4.3 RREA spectra

The supplementary material presents all the comparison spectra we obtained for photon, electrons and positrons, for the electric field between 0.80 MV/m and 2.8 MV/m. In this section, we discuss the most important differences we could find out between the four models.

4.3.1 Electrons

After the RREA electron spectra has reached self-similar state (that requires at least 5 avalanche lengths or times), we recorded the energy spectrum in a plane at a given distance (that is different for each electric field). Then we fitted it with an exponential spectrum model $\propto \exp(-\epsilon/\bar{\epsilon})$ (see also equation 8). Note that for an exponential distribution, the mean of the energy distribution is an estimator of its parameter $\bar{\epsilon}$, justifying the bar notation. We chose to evaluate the mean energy $\bar{\epsilon}$ for record at distances because, contrary to time records, it produces spectra that can be perfectly fit with an exponential distribution over the whole energy range (0 to 100 MeV). Therefore, in this case only the mean RREA electron energy is uniquely defined, and

Geosci. Model Dev. Discuss., https://doi.org/10.5194/gmd-2018-119
Manuscript under review for journal Geosci. Model Dev.
Discussion started: 14 June 2018

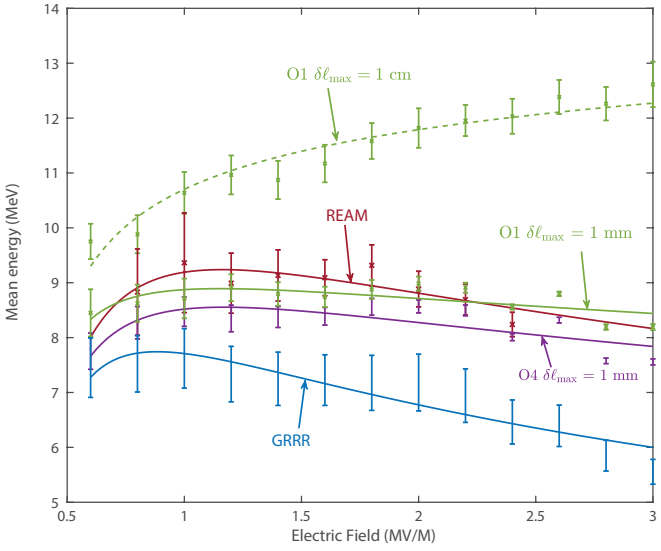

Figure 6. Mean electron energies at self-similar state (for distance record), for different electric field magnitudes. The data points are fitted with the model presented in section 4.3.1, equation 20. The values of the fitted parameters are presented in Table 2. To highlight the importance of including step limitations, Geant4 O1 values are presented for two different max step ($\delta\ell_{\max}$) settings: one that is not acceptable (1 cm) and one that is acceptable (1 mm).

does not depend on an arbitrarily chosen energy threshold, or fitting method. The mean energy $\bar{\epsilon}$ of the exponential spectrum is calculated for the several codes as a function of electric field E, as presented in figure 6. For Geant4 O1 the whole simulations and analysis were done twice, for max step length settings of $\delta\ell_{\max} = 1$ cm and $\delta\ell_{\max} = 1$ mm, to show that the first case generates totally incorrect spectra. The final data was fitted again by three parameters a_1, a_2 and a_3, following the model,

$$\bar{\epsilon}_{\text{fit}}(E) = \lambda(E)(qE - F), \quad \lambda(E) = \beta c \left[a_1 \left(\frac{qE}{F} \right)^{a_2} + a_3 \right]^{-1}, \tag{20}$$

motivated by the facts that $\epsilon_2^{\min}$ is roughly a power-law of E (see figure 2) and λ is a power-law of $\epsilon_2^{\min}$ (see equation 3). We set $F = 0.28$ MV/m, that is approximately the RREA threshold. The speed β is chosen constant, equal to 0.90, because the RREA velocity does not change of more than 5 % over the range of electric fields. The fits are in general agreement with the calculations of Celestin et al. (2012), where $\lambda(E)$ presents an approximately linear relation with the electric field. Figure 6 shows the corresponding plots, and table 2 the corresponding parameters of the fits.

In figure 6, it is clear that the Geant4 O1 model with $\delta\ell_{\max} = 1$ cm presents a significantly higher $\bar{\epsilon}(E)$ than the other codes, with values ranging from 9.5 MeV to 12.5 MeV. From the previous RREA probability simulations (see section 3), we know that this $\delta\ell_{\max}$ parameter is not low enough, and so the results of this model can be disqualified. However, when $\delta\ell_{\max}$ is reduced to 1 mm, the results of both Geant4 model are close. There seems to be a consensus between Geant4 (O1 and O4) and REAM, that gives a mean energy that is between 8 and 9 MeV and can vary up to 10 % depending on the electric field. For all

Geosci. Model Dev. Discuss., https://doi.org/10.5194/gmd-2018-119
Manuscript under review for journal Geosci. Model Dev.
Discussion started: 14 June 2018

Geoscientific Model Development Discussions
Open Access
EGU

Table 2. Mean energy variation with electric field. For evaluated codes we fitted by equation 20, with $F = 0.28$ MV/m. Figure 6 shows the corresponding curves.

Code \ Parameter	a_1 [$10^6 s^{-1}$]	a_2	a_3 [$10^6 s^{-1}$]
Geant4 O1 (δl_{max} = 1 mm)	5.96	1.14	-4.15
Geant4 O4 (δl_{max} = 1 mm)	4.99	1.23	-1.85
Geant4 O1 (δl_{max} = 1 cm)	6.96	0.929	-5.15
REAM	3.82	1.3175	-3.25×10^{-3}
GRRR	6.87	1.1760	-5.63

electric field magnitudes, GRRR shows a smaller average energy, from about 10 % less at 1 MV/m to about 20 % less at 2.8 MV/m. The reason is certainly because GRRR only includes radiative energy looses as a continuous friction. This is actually a similar difference to what has been observed and discussed in Rutjes et al. (2016) concerning the high energy electron beams, and one can read the discussion therein for more details.

Figure 7 compares the electron spectra recorded at 128 meters, for an electric field $E = 0.80$ MV/m, for a RREA generated from 200 seed electrons with $\epsilon = 100$ keV. The error bars on the bottom panel represent the uncertainty due to the Poisson statistics inherent when counting particles. The four models are consistent within 10 % between 20 keV and 7 MeV. Below 20 keV, we think the discrepancy is not physical, and can be attributed to the recording methods set up for the different codes, that are not perfect and have a more or less important uncertainty range (that is not included in the display errors bars, only based on Poisson statistics). Above 7 MeV, O1 remains consistent with REAM overall, but O4 and O1 deviate significantly : up to 50 % for O4 and up to 90 % for GRRR. For the last bin between 58 and 74 MeV, O4 and GRRR are inconsistent, that is explained by the fact that GRRR does not include straggling for Bremsstrahlung (i.e. either explicit bremsstrahlung collision or some stochastic fluctuations mimicking straggling). The deviations for the high energy part (>7 MeV) in the electron spectrum are significant for this particular field ($E = 0.80$ MV/m), however this is not true for all electric fields, where the codes are overall roughly consistent, as seen in the Supplementary Material (section 6). In principle O4 should be more precise than O1 (Allison et al., 2006), as it includes more advanced models, yet we cannot argue that O4 is more accurate than REAM. One way of deciding which model is the most accurate might be to compare these results with experimental measurements. but in the context of TGF and Gamma-ray glows it is complicated to get a proper measurement of electron spectra produced by RREA. However, photons have much longer attenuation lengths than electron and can be more easily detected, e.g. from mountains, planes, balloons or satellites. In the next section we present and discuss the corresponding photon spectra.

Geosci. Model Dev. Discuss., https://doi.org/10.5194/gmd-2018-119
Manuscript under review for journal Geosci. Model Dev.
Discussion started: 14 June 2018

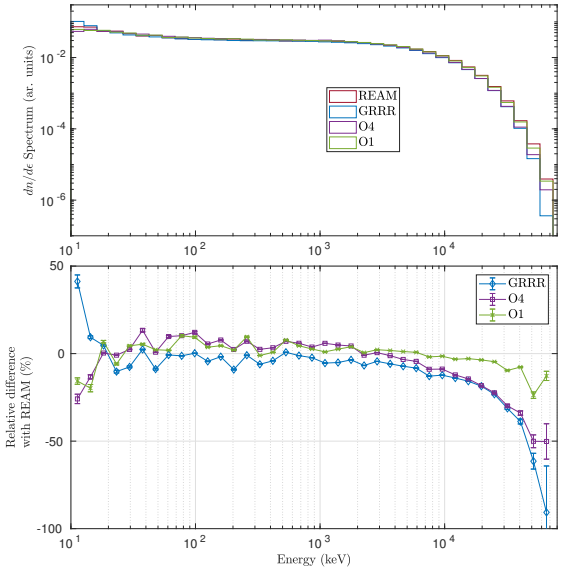

Figure 7. Top : Electron (kinetic) energy spectra of Geant4 (O4 and O1), REAM and GRRR, for $E = 0.80$ MV/m, recorded at 128 m. The RREA is generated from 200 seed electrons of $\epsilon = 100$ keV. **Bottom** : relative difference between REAM and the three other models. The error bars are calculated from the Poisson statistics.

4.3.2 Photons

In figure 8, the photon spectra recorded at 128 m for $E = 0.80$ MV/m are given for Geant4 O4/O4 and REAM, together with the relative difference with respect to REAM. The error bars in the relative differences represent the uncertainty due to the inherent Poisson statistics when evaluating particle counts. The Geant4 O1 and O4 models are consistent for the full energy range, except a small discrepancy below 20 keV, that can be attributed to different physical models, O4 being more accurate in principle. In this case, it cannot be attributed to recording methods, since they are exactly the same for both Geant4 models. At 10 keV the two Geant4 spectra are about 80 % larger than REAM. With increasing energy, the discrepancy reduces and reaches 0 % at 100 keV. Above 100 keV, the three models show consistent spectra. There may be some discrepancy above 30 MeV, but it is hard to conclude since the uncertainty interval is relatively large large.

As just presented, the main noticeable discrepancy between O1/O4 and REAM is present below 100 keV. As far as we know, there is no reason to argue that Geant4 gives a better result than REAM in this range, or vice-versa. One way to find out which model is the most accurate could be to compare these results with real measurements. Are such measurement possible to obtain? Any photon that an instrument could detect has to travel in a significant amount of air before reaching detectors. The average path travelled in the atmosphere by a 100 keV photon in 12 km altitude air is 1540 ± 806 meters. It decreases for lower energies and is 671 ± 484 meters at 50 keV, and 63.0 ± 61.5 meters at 20 keV. Therefore these photons have no chance to

Geosci. Model Dev. Discuss., https://doi.org/10.5194/gmd-2018-119
Manuscript under review for journal Geosci. Model Dev.
Discussion started: 14 June 2018

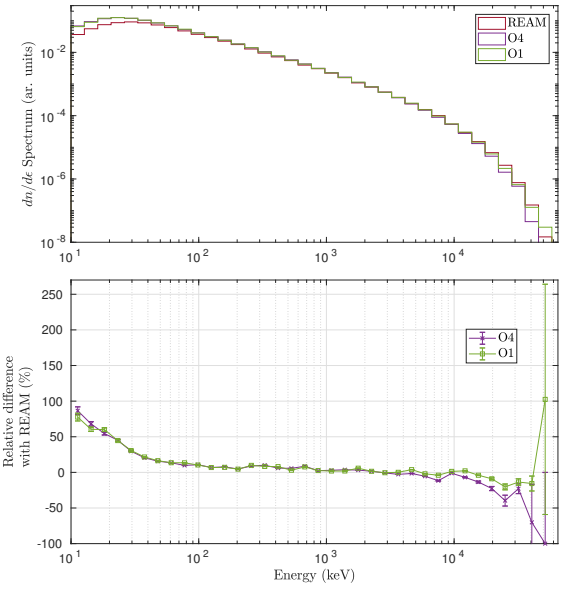

Figure 8. Top : Photon energy spectra of Geant4 (O4 and O1) and REAM for $E = 0.80$ MV/m, recorded at 128 m. **Bottom** : relative difference between Geant4 (O1 and O4) and REAM. The error bars are calculated from the Poisson statistics.

escape the atmosphere and to be detected by a satellite, but we cannot exclude that they may reach an airborne detector located inside a thunderstorm.

4.4 Other differences

In addition to what is presented so far in this article, the following points should also be mentioned when comparing the results of the codes. The corresponding plots are available in the Supplementary Material.

- The parallel velocity $\beta_{\parallel}$ (to the E-field direction) of the avalanche is shown in section 9.2 of the Supplementary Material. We observe that GRRR is giving $\beta_{\parallel}$ faster than all the other codes, and O4 is systematically slower than REAM and O1, though the differences are less than 2 %. The variation of $\beta_{\parallel}$ towards the electric field E is small, about 10 % for all codes. For increasing E-fields, electrons are less scattered and more focused in the field direction, hence slightly increasing $\beta_{\parallel}$.

- The electron to (bremsstrahlung) photon ratio $r_{e/p}$ was also calculated and compared for different distance record in the RREA shower, and the corresponding plots are presented in the Supplementary Material, section 7. GRRR is excluded because it does not include photons. For any electric field, the same discrepancy is observed. At the beginning of the shower (<4 avalanche lengths), $r_{e/p}$ appears to be about 20 % larger for REAM compared to O1 and O4, then the three models are consistent at a given distance, and finally for more than about 4 avalanche lengths, the tendency is inverted and REAM presents a $r_{e/p}$ about 20 % smaller than Geant4. The magnitude of this discrepancy is largely reduced

Geosci. Model Dev. Discuss., https://doi.org/10.5194/gmd-2018-119
Manuscript under review for journal Geosci. Model Dev.
Discussion started: 14 June 2018

Geoscientific Model Development Discussions

for increasing electric fields. We did not fully understand the reasons of these differences, and it may be due to the bremsstrahlung models used are involved. More investigations are required.

- The positron spectra have relatively low statistics (in the order of few hundreds particles recorded) and are all quite consistent within the relatively large uncertainties.
- In the photon spectra obtained from particle records at fixed times, REAM seems to show significantly less (at least a factor of 10) photon counts than the two Geant4 models for most of the electric fields magnitudes. For some fields, it even shows a lack of high energy photons, with a sharp cut at about 30 MeV. It seems to point out to a problem in the record method, explaining why we chose not to discuss these spectra in the main article. The spectra produced by the Geant4 O1 and O4 models for this case are consistent with one another for all the E-fields.

5 Conclusion

We have investigated the results of three Monte Carlo codes able to simulate Relativistic Runaway Electron Avalanches (RREA). The Monte-Carlo codes REAM, GRRR and Geant4 (two models: O1 and O4) were compared. The main difference between O4 and O1 is due to the inclusion of more precise cross sections for low energy interactions (< 10 keV). From analytical considerations, we have shown first that the full characterisation of the RREA (such as the avalanche length or the mean energy) is mainly driven by processes determining $\epsilon_2^{\min}$ (the minimum energy of electrons that can runaway) and the associated probabilities. The exact value of $\epsilon_2^{\min}$ depends on the electric field magnitude, but a reasonable lower boundary can be set to $\epsilon_2^{\min} = 10$ keV for any electric field below 3 MV/m (at STP).

To investigate this point further, we have estimated the probability to produce a RREA from a given electron energy (ϵ) and a given electric field magnitude (E). We found that the stepping methodology is of major importance, and the stepping parameters are not set up satisfactorily in Geant4 by default. We pointed out which settings should be adjusted and provided example codes to the community (see sections 6 and 7). From the Geant4 and GRRR simulations, we found that the probability for the particles below 10 keV to accelerate and participate in the penetrating radiation is actually negligible for the full range of electric field we tested ($E < 3$ MV/m). In practice, an energy threshold ε_c of about of 10 keV or higher (for lower fields) can be used, making possible to have relatively fast simulations. The advantage of using more sophisticated cross sections able to accurately track low energy particles could be probed by comparing directly O1 and O4: it showed minor differences that are mainly visible only for high E-fields ($E > 2$ MV/m), where particles with lower energies have more chance to runaway.

In a second part, we produced RREA simulations from the four models, and compared the physical characteristics of the produced RREA. The two Geant4 models and REAM showed a good agreement on all the parameters we tested. GRRR also showed an overall good agreement with the other codes, except for the electron energy spectra. As far as we know, it is probably because GRRR does not include straggling for the radiative and ionisation energy losses, hence implementing these two processes is of primary importance to produce accurate RREA spectra. By comparing O1 and O4, we also pointed out that

Geosci. Model Dev. Discuss., https://doi.org/10.5194/gmd-2018-119
Manuscript under review for journal Geosci. Model Dev.
Discussion started: 14 June 2018

including precise modelling of the interactions of particles below 10 keV provided only small differences; the most important being a $\approx 5\%$ change in the avalanche multiplication times and lengths.

6 Recommendations

From the experience of this study, we give the following general recommendations concerning RREA simulations :

- Codes should be checked / tested / benchmarked using standard test set-ups. In the supplementary material, we provide a precise description of such tests. In section 6, we provide links to download the full dataset we obtained for the codes we tested (Geant4 with two set-ups, REAM and GRRR), as well as processing scripts. We also provide the source code of the Geant4 codes.
- Custom-made codes should be make available to other researchers, or at least the results they give for standard tests.
- In order to make it possible to compare results from different studies, the methodology used to derive a given quantity should be rigorously chosen, and presented somewhere (in the main article, in the supplementary material, on a webpage, or other).
- Extending the recommendations of Rutjes et al. (2016), we concluded that to get an accurate RREA electron spectra above 10 MeV, radiative loss (bremsstrahlung) should not be implemented with uniform friction only: straggling should be included. Straggling should also be included for ionisation energy looses below threshold.

Concerning the usage of Geant4 for simulating RREA :

- Default settings are not able to simulate RREA accurately. To get accurate RREA results, one of the following tweaks is possible :
  - Changing the α_R ("dR over Range") parameter of the electron/positron ionisation process to 5.0×10^{-3} or less. This solution gives the best ratio between accuracy and computation time. Leave the "final range" parameter to one millimeter (default value) or less.
  - Setting up a step limitation process (or a maximum acceptable step) to one millimeters or less. This will significantly increase computation time.
  - Using the single (Coulomb) scattering model instead of multiple scattering. This will quite substantially increase the necessary computation time.
- In section 7, we provide link to Geant4 example source codes implementing these three methods.
- Compared to using the default Møller/Bhabha scattering models for ionisation, the usage of more accurate cross sections, e.g. taking into account the electrons' molecular biding energies (like done for the Livermore or Penelope models), only leads to minor differences.

Geosci. Model Dev. Discuss., https://doi.org/10.5194/gmd-2018-119
Manuscript under review for journal Geosci. Model Dev.
Discussion started: 14 June 2018

Geoscientific Model Development Discussions

7 Code and/or data availability

The full simulation output data of the four models is available though the following link:
https://filesender.uninett.no/?s=download&token=738a8663-a457-403a-991e-ae8d3fca3dc3

The scripts used to process this data to make the figure of the supplementary material are available in the following repository:
https://gitlab.com/dsarria/HEAP2_matlab_codes.git

The full GRRR source code is available in the following repository :
https://github.com/aluque/grrr/tree/avalanches

The Geant4 source code for the RREA probability simulations is available in the following repository :
https://gitlab.com/dsarria/av_prob.git

The Geant4 source code for the RREA characterisation simulations is available in the following repository :
https://gitlab.com/dsarria/RREA_characteristics.git

Author contributions. DS, CR and GD designed the tests. DS, CR, GD wrote most of the manuscript. DS, GD and CR proceeded to the data analysis and made the figures and tables. DS carried out the Geant4 simulations and provided the data. AL carried out the GRRR simulations and provided the data. JRD and KMAI carried out the REAM simulations and provided the data. NO, KMAI, JRD, UE, ABS and ISF provided important feedback and review on the text.

Acknowledgements.

This work was supported by the European Research Council under the European Union's Seventh Framework Program (FP7/2007-2013)/ERC grant agreement n. 320839 and the Research Council of Norway under contracts 208028/F50 and 223252/F50 (CoE). Gabriel Diniz is supported by the Brazilian agency CAPES. This material is based in part upon work supported by the Air Force Office of Scientific Research under award number FA9550-16-1-0396. For part of the results of this work, it was necessary to use the Fram computer cluster of the UNINETT Sigma2 AS, under project number NN9526K.

Appendix A: Geant4 relative performance

Table A1 presents the relative computation times it takes to complete the simulation with an Electric field magnitude of 1.2 MV/m, and 100 seed electrons with initial energy $\epsilon = 100$ keV, and a stop time (physical) of 233 nanoseconds. The fastest simulation uses Geant4 with the O1 physics list and $\delta\ell_{\max} = 10$ cm and took 4.53 seconds to complete on one thread with the microprocessor we used. The simulations with the O4 physics list with $\delta\ell_{\max} = 1$ mm requires about 400 times more computation time. Setting up $\delta\ell_{\max} = 1$ mm, or lower, is necessary to achieve correct simulation of the RREA process, as argued in section 3. To achieve it for the full range of electric fields we tested (in a reasonable amount of time), it required the use of the Norwegian FRAM computer cluster. The simulations with $\delta\ell_{\max} = 0.1$ mm for all electric fields could not be achieved in a reasonable amount of time, even by using the computer cluster.

Geosci. Model Dev. Discuss., https://doi.org/10.5194/gmd-2018-119
Manuscript under review for journal Geosci. Model Dev.
Discussion started: 14 June 2018

Geoscientific Model Development Discussions

Model / $\delta\ell_{\max}$	Option 1 (O1)	Option 4 (O4)
10 cm	**1**	**6.49**
1 cm	**11.5**	**27.2**
1 mm	**222**	**393**
0.1 mm	**2100**	**3740**
α_R (default)	0.80	0.20

Model / α_R	Option 1 (O1)	Option 4 (O4)
0.80	**≈1**	**2.44**
0.20	**2.61**	**7.66**
0.050	**7.12**	**36.5**
0.0050	**21.0**	**126**
0.0010	**41.7**	**224**
$\delta\ell_{\max}$ (default)	1 km	1 km

Table 3. Computation time needed by different Geant4 configurations for the simulation of the same physical problem, relatively to the Geant4 O1 $\delta\ell_{\max} = 10$ cm case. Two parameters are tested : the maximum allowed step ($\delta\ell_{\max}$) and the "dRoverRange" (α_R).

On the other hand, if $\delta\ell_{\max}$ is left at its default value (1 kilometer) and α_R parameter is tweaked instead, accurate simulations can be achieved with a value of $\alpha_R = 5.0 \times 10^{-3}$ or lower. It requires almost an order of magnitude less computation time compared to using $\delta\ell_{\max} = 1$ mm.

References

Adachi, T., Takahashi, Y., Ohya, H., Tsuchiya, F., Yamashita, K., Yamamoto, M., and Hashiguchi, H.: Monitoring of Lightning Activity in Southeast Asia: Scientific Objectives and Strategies, Kyoto Working Papers on Area Studies: G-COE Series, 2008.

Agostinelli, S. et al.: GEANT4: A simulation toolkit, Nucl. Instrum. Meth., A506, 250–303, doi:10.1016/S0168-9002(03)01368-8, 2003.

Allison, J., Amako, K., Apostolakis, J., Araujo, H., Dubois, P. A., Asai, M., Barrand, G., Capra, R., Chauvie, S., Chytracek, R., Cirrone, G. A. P., Cooperman, G., Cosmo, G., Cuttone, G., Daquino, G. G., Donszelmann, M., Dressel, M., Folger, G., Foppiano, F., Generowicz, J., Grichine, V., Guatelli, S., Gumplinger, P., Heikkinen, A., Hrivnacova, I., Howard, A., Incerti, S., Ivanchenko, V., Johnson, T., Jones, F., Koi, T., Kokoulin, R., Kossov, M., Kurashige, H., Lara, V., Larsson, S., Lei, F., Link, O., Longo, F., Maire, M., Mantero, A., Mascialino, B., McLaren, I., Lorenzo, P. M., Minamimoto, K., Murakami, K., Nieminen, P., Pandola, L., Parlati, S., Peralta, L., Perl, J., Pfeiffer, A., Pia, M. G., Ribon, A., Rodrigues, P., Russo, G., Sadilov, S., Santin, G., Sasaki, T., Smith, D., Starkov, N., Tanaka, S., Tcherniaev, E., Tome, B., Trindade, A., Truscott, P., Urban, L., Verderi, M., Walkden, A., Wellisch, J. P., Williams, D. C., Wright, D., and Yoshida, H.: Geant4 developments and applications, IEEE Transactions on Nuclear Science, 53, 270–278, doi:10.1109/TNS.2006.869826, 2006.

Allison, J., Amako, K., Apostolakis, J., et al.: Recent developments in Geant4, Nuclear Instruments and Methods in Physics Research Section A: Accelerators, Spectrometers, Detectors and Associated Equipment, 835, 186 – 225, doi:https://doi.org/10.1016/j.nima.2016.06.125, http://www.sciencedirect.com/science/article/pii/S0168900216306957, 2016.

Apostolakis, J., Asai, M., Bogdanov, A., Burkhardt, H., Cosmo, G., Elles, S., Folger, G., Grichine, V., Gumplinger, P., Heikkinen, A., Hrivnacova, I., Ivanchenko, V., Jacquemier, J., Koi, T., Kokoulin, R., Kossov, M., Kurashige, H., McLaren, I., Link, O., Maire, M., Pokorski, W., Sasaki, T., Starkov, N., Urban, L., and Wright, D.: Geometry and physics of the Geant4 toolkit for high and medium energy applications, Radiation Physics and Chemistry, 78, 859 – 873, doi:https://doi.org/10.1016/j.radphyschem.2009.04.026, http://www.sciencedirect.com/science/article/pii/S0969806X09001650, workshop on Use of Monte Carlo Techniques for Design and Analysis of Radiation Detectors, 2009.

Babich, L., Donskoy, E., Kutsyk, I., and Roussel-Dupré, R.: The feedback mechanism of runaway air breakdown, Geophysical research letters, 32, L09809, doi:10.1029/2004GL021744, 2005.

Babich, L. P., Donskoy, E. N., Kutsyk, I. M., Kudryavtsev, A. Y., Roussel-Dupre, R. A., Shamraev, B. N., and Symbalisty, E. M.: Comparison of relativistic runaway electron avalanche rates obtained from Monte Carlo simulations and kinetic equation solution, IEEE transactions on plasma science, 29, 430–438, 2001.

Bethe, H. and Heitler, W.: On the stopping of fast particles and on the creation of positive electrons, Proceedings of the Royal Society of London A: Mathematical, Physical and Engineering Sciences, 146, 83–112, 1934.

Bowers, G. S., Smith, D. M., Martinez-McKinney, G., Kamogawa, M., Cummer, S., Dwyer, J., Wang, D., Stock, M., and Kawasaki, Z.: Gamma Ray Signatures of Neutrons From a Terrestrial Gamma Ray Flash, Geophysical Research Letters, 2017.

Briggs, M. S., Fishman, G. J., Connaughton, V., Bhat, P. N., Paciesas, W. S., Preece, R. D., Wilson-Hodge, C., Chaplin, V. L., Kippen, R. M., von Kienlin, A., Meegan, C. A., Bissaldi, E., Dwyer, J. R., Smith, D. M., Holzworth, R. H., Grove, J. E., and Chekhtman, A.: First results on terrestrial gamma ray flashes from the Fermi Gamma-ray Burst Monitor, Journal of Geophysical Research (Space Physics), 115, A07323, doi:10.1029/2009JA015242, 2010.

Briggs, M. S., Connaughton, V., Wilson-Hodge, C., Preece, R. D., Fishman, G. J., Kippen, R. M., Bhat, P., Paciesas, W. S., Chaplin, V. L., Meegan, C. A., et al.: Electron-positron beams from terrestrial lightning observed with Fermi GBM, Geophysical research letters, 38, L02808, doi:10.1029/2010GL046259, 2011.

Brown, J. M. C., Dimmock, M. R., Gillam, J. E., and Paganin, D. M.: A low energy bound atomic electron Compton scattering model for Geant4, Nuclear Instruments and Methods in Physics Research B, 338, 77–88, doi:10.1016/j.nimb.2014.07.042, 2014.

Carlson, B., Lehtinen, N. G., and Inan, U. S.: Neutron production in terrestrial gamma ray flashes, Journal of Geophysical Research: Space Physics, 115, A00E19, doi:10.1029/2009JA014696, 2010.

Celestin, S. and Pasko, V. P.: Soft collisions in relativistic runaway electron avalanches, Journal of Physics D: Applied Physics, 43, 315206, doi:10.1088/0022-3727/43/31/315206, 2010.

Celestin, S. and Pasko, V. P.: Energy and fluxes of thermal runaway electrons produced by exponential growth of streamers during the stepping of lightning leaders and in transient luminous events, Journal of Geophysical Research: Space Physics, 116, A03315, doi:10.1029/2010JA016260, 2011.

Celestin, S., Xu, W., and Pasko, V. P.: Terrestrial gamma ray flashes with energies up to 100 MeV produced by nonequilibrium acceleration of electrons in lightning, Journal of Geophysical Research (Space Physics), 117, A05315, doi:10.1029/2012JA017535, http://dx.doi.org/10.1029/2012JA017535, a05315, 2012.

Chanrion, O. and Neubert, T.: Production of runaway electrons by negative streamer discharges, J. Geophys. Res. (Space Phys), 115, A00E32, doi:10.1029/2009JA014774, 2010.

Chanrion, O., Bonaventura, Z., Çinar, D., Bourdon, A., and Neubert, T.: Runaway electrons from a "beam-bulk" model of streamer: application to TGFs, Environmental Research Letters, 9, 055003, doi:10.1088/1748-9326/9/5/055003, 2014.

Chanrion, O., Bonaventura, Z., Bourdon, A., and Neubert, T.: Influence of the angular scattering of electrons on the runaway threshold in air, Plasma Physics and Controlled Fusion, 58, 044 001, 2016.

Chilingarian, A., Daryan, A., Arakelyan, K., Hovhannisyan, A., Mailyan, B., Melkumyan, L., Hovsepyan, G., Chilingaryan, S., Reymers, A., and Vanyan, L.: Ground-based observations of thunderstorm-correlated fluxes of high-energy electrons, gamma rays, and neutrons, Physical Review D, 82, 043009, doi:10.1103/PhysRevD.82.043009, 2010.

Chilingarian, A., Hovsepyan, G., and Hovhannisyan, A.: Particle bursts from thunderclouds: Natural particle accelerators above our heads, Physical review D, 83, 062001, doi:10.1103/PhysRevD.83.062001, 2011.

Chilingarian, A., Hovsepyan, G., Khanikyanc, G., Reymers, A., and Soghomonyan, S.: Lightning origination and thunderstorm ground enhancements terminated by the lightning flash, EPL (Europhysics Letters), 110, 49 001, 2015.

Coleman, L. M. and Dwyer, J. R.: Propagation speed of runaway electron avalanches, Geophysical Research Letters, 33, L11810, doi:10.1029/2006GL025863, 2006.

Cramer, E. S., Dwyer, J. R., Arabshahi, S., Vodopiyanov, I., Liu, N., and Rassoul, H.: An analytical approach for calculating energy spectra of relativistic runaway electron avalanches in air, Journal of Geophysical Research: Space Physics, 119, 7794–7823, 2014.

Cramer, E. S., Dwyer, J. R., and Rassoul, H. K.: Magnetic field modification to the relativistic runaway electron avalanche length, Journal of Geophysical Research (Space Physics), 121, 11, doi:10.1002/2016JA022891, 2016.

Dubinova, A., Rutjes, C., Ebert, U., Buitink, S., Scholten, O., and Trinh, G. T. N.: Prediction of Lightning Inception by Large Ice Particles and Extensive Air Showers, Physical Review Letters, 115, 015 002, doi:10.1103/PhysRevLett.115.015002, https://link.aps.org/doi/10.1103/PhysRevLett.115.015002, 2015.

Dwyer, J. R.: A fundamental limit on electric fields in air, Geophysical Research Letters, 30, 2055, doi:10.1029/2003GL017781, http://www.agu.org/pubs/crossref/2003/2003GL017781.shtml, 2003.

Dwyer, J. R.: Relativistic breakdown in planetary atmospheres, Physics of Plasmas, 14, 042 901, doi:10.1063/1.2709652, 2007.

Dwyer, J. R.: Source mechanisms of terrestrial gamma-ray flashes, Journal of Geophysical Research: Atmospheres, 113, n/a–n/a, doi:10.1029/2007JD009248, http://dx.doi.org/10.1029/2007JD009248, d10103, 2008.

Dwyer, J. R.: The relativistic feedback discharge model of terrestrial gamma ray flashes, J. Geophys. Res. (Space Phys), 117, A02308, doi:10.1029/2011JA017160, 2012.

Dwyer, J. R., Grefenstette, B. W., and Smith, D. M.: High-energy electron beams launched into space by thunderstorms, Geophysical Research Letters, 35, L02815, doi:10.1029/2007GL032430, http://dx.doi.org/10.1029/2007GL032430, 2008.

Dwyer, J. R., Smith, D. M., and Cummer, S. A.: High-Energy Atmospheric Physics: Terrestrial Gamma-Ray Flashes and Related Phenomena, Space Science Review, 173, 133–196, doi:10.1007/s11214-012-9894-0, 2012.

Eack, K. B., Beasley, W. H., Rust, W. D., Marshall, T. C., and Stolzenburg, M.: Initial results from simultaneous observation of X-rays and electric fields in a thunderstorm, Journal of Geophysical Research: Atmospheres, 101, 29 637–29 640, doi:10.1029/96JD01705, 1996.

Ferrari, A., Sala, P. R., Fasso, A., and Ranft, J.: FLUKA: A multi-particle transport code (Program version 2005), Tech. rep., 2005.

Fishman, G. J., Bhat, P. N., Mallozzi, R., Horack, J. M., Koshut, T., Kouveliotou, C., Pendleton, G. N., Meegan, C. A., Wilson, R. B., Paciesas, W. S., Goodman, S. J., and Christian, H. J.: Discovery of Intense Gamma-Ray Flashes of Atmospheric Origin, Science, 264, 1313–1316, doi:10.1126/science.264.5163.1313, 1994.

Gurevich, A.: On the theory of runaway electrons, Sov. Phys. JETP, 12, 904–912, 1961.

Gurevich, A. and Zybin, K.: Kinetic equation for high energy electrons in gases, Physics Letters A, 237, 240–246, 1998.

Gurevich, A., Milikh, G., and Roussel-Dupre, R.: Runaway electron mechanism of air breakdown and preconditioning during a thunderstorm, Physics Letters A, 165, 463–468, doi:10.1016/0375-9601(92)90348-P, http://linkinghub.elsevier.com/retrieve/pii/037596019290348P, 1992.

Hirayama, H., Namito, Y., Nelson, W. R., Bielajew, A. F., Wilderman, S. J., and Michigan, U.: The EGS5 code system, Tech. rep., United States. Department of Energy, 2005.

Ivanchenko, V. N., Bukin, A. D., Dubrovin, M. S., Eidelman, S. I., Grozina, N. A., and Tayursky, V. A.: UNIMOD2: Universal Monte Carlo code for simulation of e+ e- experiments, in: MC 91: Detector and event simulation in high-energy physics. Proceedings, Workshop, Amsterdam, Netherlands, April 8-12, 1991, pp. 79–85, 1991.

Kelley, N. A., Smith, D. M., Dwyer, J. R., Splitt, M., Lazarus, S., Martinez-McKinney, F., Hazelton, B., Grefenstette, B., Lowell, A., and Rassoul, H. K.: Relativistic electron avalanches as a thunderstorm discharge competing with lightning, Nature communications, 6, 2015.

Kochkin, P., van Deursen, A. P. J., Marisaldi, M., Ursi, A., de Boer, A. I., Bardet, M., Allasia, C., Boissin, J.-F., Flourens, F., and Østgaard, N.: In-flight observation of gamma-ray glows by ILDAS, Journal of Geophysical Research: Atmospheres, doi:10.1002/2017JD027405, http://dx.doi.org/10.1002/2017JD027405, 2017.

Köhn, C. and Ebert, U.: Calculation of beams of positrons, neutrons, and protons associated with terrestrial gamma ray flashes, Journal of Geophysical Research: Atmospheres, 120, 1620–1635, 2015.

Kohn, C., Ebert, U., and Mangiarotti, A.: The importance of electron–electron bremsstrahlung for terrestrial gamma-ray flashes, electron beams and electron–positron beams, Journal of Physics D: Applied Physics, 47, 252 001, http://stacks.iop.org/0022-3727/47/i=25/a=252001, 2014.

Köhn, C., Diniz, G., and Harakeh, M. N.: Production mechanisms of leptons, photons, and hadrons and their possible feedback close to lightning leaders, Journal of Geophysical Research: Atmospheres, 122, 1365–1383, 2017.

Landau, L. D., Bell, J., Kearsley, M., Pitaevskii, L., Lifshitz, E., and Sykes, J.: Electrodynamics of continuous media, vol. 8, elsevier, 2013.

Lefeuvre, F., Blanc, E., and Pinçon, J. L.: TARANIS-a Satellite Project Dedicated to the Physics of TLEs and TGFs, in: American Institute of Physics Conference Series, vol. 1118 of *American Institute of Physics Conference Series*, pp. 3–7, doi:10.1063/1.3137711, 2009.

Lehtinen, N. G., Bell, T. F., and Inan, U. S.: Monte Carlo simulation of runaway MeV electron breakdown with application to red sprites and terrestrial gamma ray flashes, jgr, 104, 24 699–24 712, doi:10.1029/1999JA900335, 1999.

Li, C., Ebert, U., and Hundsdorfer, W.: 3D hybrid computations for streamer discharges and production of runaway electrons, Journal of Physics D: Applied Physics, 42, 202003, doi:10.1088/0022-3727/42/20/202003, 2009.

Liu, C., Brennan, D. P., Bhattacharjee, A., and Boozer, A. H.: Adjoint Fokker-Planck equation and runaway electron dynamics, Physics of Plasmas, 23, 010 702, 2016.

Luque, A.: Relativistic Runaway Ionization Fronts, Physical Review Letters, 112, 045003, doi:10.1103/PhysRevLett.112.045003, 2014.

McCarthy, M. and Parks, G.: Further observations of X-rays inside thunderstorms, Geophysical Research Letters, 12, 393–396, doi:10.1029/GL012i006p00393, 1985.

Moss, G. D., Pasko, V. P., Liu, N., and Veronis, G.: Monte Carlo model for analysis of thermal runaway electrons in streamer tips in transient luminous events and streamer zones of lightning leaders, Journal of Geophysical Research (Space Physics), 111, A02307, doi:10.1029/2005JA011350, 2006.

Neubert, T., Kuvvetli, I., Budtz-Jørgensen, C., Østgaard, N., Reglero, V., and Arnold, N.: The atmosphere-space interactions monitor (ASIM) for the international space station, in: Proceedings of the ILWS Workshop, edited by Gopalswamy, N. and Bhattacharyya, A., p. 448, 2006.

Østgaard, N., Gjesteland, T., Stadsnes, J., Connell, P., and Carlson, B.: Production altitude and time delays of the terrestrial gamma flashes: Revisiting the Burst and Transient Source Experiment spectra, Journal of Geophysical Research: Space Physics, 113, A02307, doi:10.1029/2007JA012618, 2008.

Perkins, S. T., Cullen, D. E., and Seltzer, S. M.: Tables and graphs of electron-interaction cross sections from 10 eV to 100 GeV derived from the LLNL Evaluated Electron Data Library (EEDL), Z = 1 to 100, Tech. rep., 1991.

Roussel-Dupre, R., Gurevich, A., Tunnell, T., and Milikh, G.: Kinetic theory of runaway air breakdown, Physical review E, 49, 2257, 1994.

Rutjes, C., Sarria, D., Skeltved, A. B., Luque, A., Diniz, G., Østgaard, N., and Ebert, U.: Evaluation of Monte Carlo tools for high energy atmospheric physics, Geoscientific Model Development, 9, 3961, doi:10.5194/gmd-9-3961-2016, http://www.geosci-model-dev.net/9/3961/2016/, 2016.

Rutjes, C., Diniz, G., Ferreira, I. S., and Ebert, U.: TGF afterglows: a new radiation mechanism from thunderstorms, Geophysical Research Letters, doi:10.1002/2017GL075552, 2017.

Salvat, F., Fernández-Varea, J. M., and Sempau, J.: PENELOPE-2011: A Code System for Monte Carlo Simulation of Electron and Photon Transport, 2011.

Sarria, D., Blelly, P.-L., and Forme, F.: MC-PEPTITA: a Monte Carlo model for Photon, Electron and Positron Tracking In Terrestrial Atmosphere. Application for a Terrestrial Gamma-ray Flash, Journal of Geophysical Research: Space Physics, pp. n/a–n/a, doi:10.1002/2014JA020695, http://dx.doi.org/10.1002/2014JA020695, 2014JA020695, 2015.

Sarria, D., Blelly, P.-L., Briggs, M. S., and Forme, F.: Studying the time histogram of a terrestrial electron beam detected from the opposite hemisphere of its associated TGF, Journal of Geophysical Research: Space Physics, pp. n/a–n/a, doi:10.1002/2015JA021881, http://dx.doi.org/10.1002/2015JA021881, 2016.

Sarria, D., Lebrun, F., Blelly, P.-L., Chipaux, R., Laurent, P., Sauvaud, J.-A., Prech, L., Devoto, P., Pailot, D., Baronick, J.-P., and Lindsey-Clark, M.: TARANIS XGRE and IDEE detection capability of terrestrial gamma-ray flashes and associated electron beams, Geoscientific

Instrumentation, Methods and Data Systems, 6, 239–256, doi:10.5194/gi-6-239-2017, https://www.geosci-instrum-method-data-syst.net/6/239/2017/, 2017.

Skeltved, A. B., Østgaard, N., Carlson, B., Gjesteland, T., and Celestin, S.: Modeling the relativistic runaway electron avalanche and the feedback mechanism with GEANT4, Journal of Geophysical Research: Space Physics, 119, 9174–9191, doi:10.1002/2014ja020504, http://dx.doi.org/10.1002/2014JA020504, 2014.

Teruaki, E., Wada, Y., et al.: Photonuclear reactions triggered by lightning discharge, Nature, 551, doi:10.1038/nature24630, https://www.nature.com/articles/nature24630, 2017.

Torii, T., Takeishi, M., and Hosono, T.: Observation of gamma-ray dose increase associated with winter thunderstorm and lightning activity, Journal of Geophysical Research: Atmospheres, 107, 4324, doi:10.1029/2001JD000938, 2002.

Tsuchiya, H., Enoto, T., Yamada, S., Yuasa, T., Kawaharada, M., Kitaguchi, T., Kokubun, M., Kato, H., Okano, M., Nakamura, S., et al.: Detection of high-energy gamma rays from winter thunderclouds, Physical review letters, 99, 165002, doi:10.1103/PhysRevLett.99.165002, 2007.

Williams, E. R.: Origin and context of C. T. R. Wilson's ideas on electron runaway in thunderclouds, Journal of Geophysical Research (Space Physics), 115, A00E50, doi:10.1029/2009JA014581, 2010.

Wilson, C. T. R.: The Acceleration of β-particles in Strong Electric Fields such as those of Thunderclouds, Proceedings of the Cambridge Philosophical Society, 22, 534, doi:10.1017/S0305004100003236, 1925.